Magnetic Resonance in Medicine 57:1196–1202 (2007)

Joint Image Reconstruction and Sensitivity Estimation in SENSE (JSENSE)

Leslie Ying* and Jinhua Sheng

Parallel magnetic resonance imaging (pMRI) using multichannel receiver coils has emerged as an effective tool to reduce imaging time in various applications. However, the issue of accurate estimation of coil sensitivities has not been fully addressed, which limits the level of speed enhancement achievable with the technology. The self-calibrating (SC) technique for sensitivity extraction has been well accepted, especially for dynamic imaging, and complements the common calibration technique that uses a separate scan. However, the existing method to extract the sensitivity information from the SC data is not accurate enough when the number of data is small, and thus erroneous sensitivities affect the reconstruction quality when they are directly applied to the reconstruction equation. This paper considers this problem of error propagation in the sequential procedure of sensitivity estimation followed by image reconstruction in existing methods, such as sensitivity encoding (SENSE) and simultaneous acquisition of spatial harmonics (SMASH), and reformulates the image reconstruction problem as a joint estimation of the coil sensitivities and the desired image, which is solved by an iterative optimization algorithm. The proposed method was tested on various data sets. The results from a set of in vivo data are shown to demonstrate the effectiveness of the proposed method, especially when a rather large net acceleration factor is used. Magn Reson Med 57: 1196–1202, 2007. © 2007 Wiley-Liss, Inc.

Key words: joint estimation; SENSE; self calibration; variable density acquisition; sensitivity estimation

Parallel magnetic resonance imaging (pMRI), as a fast imaging method, uses an array of RF receiver surface coils to acquire multiple sets of undersampled *k*-space data simultaneously. Over the past few years a number of pMRI techniques have been proposed for reconstructing a complete MR image from these undersampled data in either *k*-space or the image domain. Some of these methods, such as partially parallel imaging with localized sensitivities (PILS) (1), auto simultaneous acquisition of spatial harmonics (AUTO-SMASH) (2), variable density (VD)-AUTO-SMASH (3), and generalized autocalibrating partially parallel acquisitions (GRAPPA) (4), do not need the explicit functions of coil sensitivity, while others, such as SMASH (5), sensitivity encoding (SENSE) (6), and sensitivity profiles from an array of coils for encoding and reconstruction in parallel (SPACE-RIP) (7), require the functions to be given exactly. For the methods in the latter category, the sensitivity estimation method is as important as the reconstruction algorithm (8).

Unfortunately, the existing techniques for determining sensitivity functions are not yet satisfactory. The most common technique has been to derive sensitivities directly from a set of reference images obtained in a separate calibration scan before or after the accelerated scans. This calibration scan can prolong the total imaging time, partially counteracting the benefits of reduced acquisition time associated with pMRI. Another practical problem with this technique is that misregistrations or inconsistencies between the calibration scan and the accelerated scan result in artifacts in the reconstructed images, which is a major concern in dynamic imaging applications. Adaptive sensitivity estimation (9,10) has been proposed for these applications. Based solely on the data from accelerated scans, the method uses unaliasing by Fourier-encoding the overlaps using the temporal dimension (UNFOLD) (11) to generate low-temporal-resolution, aliasing-free reference images for sensitivity estimation. However, UNFOLD is limited to dynamic applications in which at least half of the field of view (FOV) remains static over time. A more general method is the self-calibrating (SC) technique, which also eliminates a separate calibration scan but acquires VD *k*-space data during the accelerated scan (8). The VD acquisition includes a small number of fully sampled lines at the center of *k*-space, known as autocalibration signal (ACS) lines, in addition to the down-sampled lines at outer *k*-space. These central *k*-space lines after Fourier transformation produce low-resolution in vivo reference images $[\rho(\vec{r})s_l(\vec{r})]*h(\vec{r})$, where the product of the coil sensitivity $S_l(\vec{r})$ of the lth channel and the image of transverse magnetization $\rho(\vec{r})$ is convolved (*) with $h(\vec{r})$, the Fourier transform of the truncation window that truncates the central *k*-space. The convolution is due to the use of only the central *k*-space data, which results in a low-resolution measurement. To derive the sensitivities, these low-resolution reference images are divided by their sum-of-squares (SoS) combination (8,12):

$$\hat{s}_l(\vec{r}) \approx \frac{[\rho(\vec{r})s_l(\vec{r})]*h(\vec{r})}{\sqrt{\Sigma_l|[\rho(\vec{r})s_l(\vec{r})]*h(\vec{r})|^2}} \qquad [1]$$

In addition to the assumption of spatially uniform $\sqrt{\Sigma_l|[s_l(\vec{r})|^2}$, which is in common with the calibrating technique with a separate scan, Eq. [1] also assumes that the multiplication with $s_l(\vec{r})$ and the convolution with $h(\vec{r})$ are commute, i.e.,

$$[\rho(\vec{r})s_l(\vec{r})]*h(\vec{r}) \approx [\rho(\vec{r})*h(\vec{r})]s_l(\vec{r}). \qquad [2]$$

where equality holds only if $h(\vec{r})$ is a Dirac delta function, i.e., when there is no data truncation, or $s_l(\vec{r})$ is spatially a

Department of Electrical Engineering and Computer Science, University of Wisconsin–Milwaukee, Milwaukee, Wisconsin, USA.

Grant sponsor: Wisconsin Institute for Biomedical and Health Technologies.

*Correspondence to: Professor L. Ying, Department of Electrical Engineering and Computer Science, University of Wisconsin–Milwaukee, 3200 N. Cramer St., Milwaukee, WI 53211. E-mail: leiying@uwm.edu

Received 25 May 2006; revised 20 December 2006; accepted 21 February 2007.

DOI 10.1002/mrm.21245

Published online in Wiley InterScience (www.interscience.wiley.com).

constant. In general, the approximation in Eq. [2] requires $s_l(\vec{r})$ to be much smoother than $h(\vec{r})$, i.e., the range of spatial frequencies covered in the ACS lines is much broader than the spatial frequency band of the coil sensitivity functions (13); however, this contradicts the goal of pMRI. Apodization of the central k-space data can also be used to shape $h(\vec{r})$ for a better approximation in Eq. [2] (8). If a small number of ACS lines are used, suggesting large data truncation, the approximation in Eq. [2] fails such that the Gibbs ringing artifacts due to truncation in the reference images cannot be canceled by the division of their SoS combination described in Eq. [1]. This leads to the presence of truncation errors in all sensitivity functions, which become serious especially at locations where the object transverse magnetization has high-spatial-frequency components. These ringing errors can hardly be reduced by the commonly used polynomial-fitting (6) or wavelet-denoising techniques (14) for sensitivities. Consequently, the pMRI reconstruction suffers from aliasing artifacts. Therefore, to improve the sensitivity accuracy with a small number of ACS data is crucial for pMRI techniques to achieve a high acceleration.

In this paper we propose a novel approach that jointly estimates the coil sensitivities and reconstructs the desired image, in contrast to the sequential sensitivity estimation followed by image reconstruction in conventional techniques. In particular, the proposed method addresses the issue of sensitivity errors by iteratively correcting the sensitivity functions using all acquired VD k-space data instead of only ACS lines. Extending the linear formulation of generalized SENSE (GSENSE) with VD data (6,15), the image reconstruction problem is reformulated as a nonlinear optimization problem, with the sensitivity functions represented by a parametric model with a set of unknown parameters. In solving the optimization problem, an iterative method is used. Specifically, starting with an initial estimation of coil sensitivities, the method alternately updates the reconstructed images and the coil sensitivity functions in each iteration, and repeats until convergence. The reconstruction results from a set of in vivo brain data are given in this paper to demonstrate its superior quality compared to SC GSENSE.

THEORY

Formulation of GSENSE

In GSENSE with VD acquisition, the imaging equation can be formulated as a linear operation of the transverse magnetization image (6,15):

$$\mathbf{E}\mathbf{f}=\mathbf{d}, \qquad [3]$$

where $\mathbf{d}$ is the vector formed from all k-space data acquired at all channels, and $\mathbf{f}$ is the unknown vector formed from the desired full-FOV image to be solved for. The encoding matrix $\mathbf{E}$ consists of the product of Fourier encoding with subsampled k-space and coil-specific sensitivity modulation over the image, i.e.,

$$\mathbf{E}_{\{l,m\},n} = e^{-i2\pi\vec{k}_m\cdot\vec{r}_n} s_l(\vec{r}_n), \qquad [4]$$

where m and n denote the indices for the k-space data and image pixels, respectively. In image reconstruction, the image $\mathbf{f}$ is solved by the least-squares method either directly (7,8) or iteratively (15,17), given knowledge of acquired data $\mathbf{d}$ and sensitivities $s_l(\vec{r})$, where the sensitivities are usually estimated by Eq. [1] and directly plugged into the reconstruction algorithms. With this sequential processing, any inaccuracy in sensitivity estimation can propagate to the reconstructed image.

Formulation of Proposed JSENSE

To improve the accuracy of sensitivity estimation using ACS data, we propose a novel method that jointly estimates the sensitivities and SENSE reconstruction (called JSENSE). The method is based on VD acquisition with both the ACS data and the reduced data used for reconstruction. In JSENSE, instead of assuming that the sensitivity functions estimated from the ACS data are exactly accurate, we introduce some degree of uncertainty. Specifically, noting the encoding matrix $\mathbf{E}$ is a function of sensitivity, the imaging equation in Eq. [3] becomes

$$\mathbf{E}(\mathbf{a})\mathbf{f}=\mathbf{d}, \qquad [5]$$

where $\mathbf{a}$ is the parameter representing the coil sensitivities and is also an unknown to be solved. Although there can be different ways to parameterize the sensitivities, we use a simple polynomial function to model the coil sensitivities as

$$s_l(\vec{r}) = \sum_{i=0}^{N}\sum_{j=0}^{N} a_{l,i,j}(x-\bar{x})^i(y-\bar{y})^j, \qquad [6]$$

where $(x,y) = \vec{r}$ denotes the location of a pixel, $(\bar{x},\bar{y})$, denotes the averaged location, and $a_{l,i,j}$ is the coefficient of a polynomial, forming the unknown vector $\mathbf{a}$. We choose the highest power of x and y to be the same and define it as the order of the polynomial. A high-order polynomial improves the accuracy of the model, but also increases the number of unknowns to be solved for. Because of the smooth nature of coil sensitivity in general, a polynomial of low order is usually sufficient. Under this model, the encoding matrix explicitly becomes

$$\mathbf{E}(\mathbf{a})_{\{l,m\},n} = \sum_{i,j} a_{l,i,j}(x_n-\bar{x})^i(y_n-\bar{y})^j e^{-i2\pi(k_{xm}\cdot x_n + k_{ym}\cdot y_n)}. \qquad [7]$$

Taking into account the k-space data noise, which is usually additive white Gaussian, we can jointly estimate the coefficients for coil sensitivities $\mathbf{a}$ and the desired image $\mathbf{f}$ by finding a least-squares solution. Specifically,

$$\{\mathbf{a},\mathbf{f}\} = \arg\min_{\{\mathbf{a},\mathbf{f}\}} \mathbf{U}(\mathbf{a},\mathbf{f}), \qquad [8]$$

where the cost function to be minimized is

$$\mathbf{U}(\mathbf{a},\mathbf{f}) = \frac{1}{2}\|\mathbf{d} - \mathbf{E}(\mathbf{a})\mathbf{f}\|^2. \quad [9]$$

Since the polynomial model already incorporates the smoothness constraint, no regularization is needed on sensitivity functions. Theoretically, as long as the dimension of data **d** exceeds the total dimension of the unknowns **a** and **f**, the above least-squares problem is overdetermined and thus has a unique solution. The novel nonlinear formulation of image reconstruction allows the sensitivity and the image to be estimated simultaneously, and thus prevents the errors of the independently estimated sensitivities from propagating to the final reconstruction as in conventional SENSE.

Implementation of JSENSE

Directly solving the joint optimization problem in Eq. [8] is practically intractable. We resort to a greedy iterative algorithm (16). Specifically, starting with an initial estimate of sensitivities by Eq. [1] using the ACS data, we alternate between updating the image and updating the polynomial coefficients of the coil sensitivities, both based on the optimization criterion in Eq. [8]. This updating procedure is repeated iteratively until the cost function stops decreasing. The corresponding image reconstructed at the final iteration gives the desired image.

To update the image, we fix the sensitivity functions to be the ones given by the previous iteration. Thus the image **f** can be reconstructed by minimizing Eq. [9]:

$$\mathbf{f} = \min_{\mathbf{f}} \frac{1}{2}\|\mathbf{d} - \mathbf{E}\mathbf{f}\|^2, \quad [10]$$

with **E** given by fixing **a**. Equation [10] becomes the same as the formulation of GSENSE with regularization (12,18). The solution is then found by the iterative conjugate gradient method, as described in detail in Ref. 15. Other image reconstruction methods that are applicable to VD acquisition, such as SPACE-RIP (7), projection onto convex set based SENSE (POCSENSE) (17), and VD-SENSE (10,19), can also be used. Even the efficient Cartesian SENSE method (6) can be used for the reconstruction component, but it is expected to have degraded image quality because the ACS data are not used.

Similarly, to update the sensitivity functions, the image is fixed. Specifically, we minimize the cost in Eq. [9] with respect to the coefficients **a** given **f**:

$$\mathbf{a} = \min_{\mathbf{a}} \frac{1}{2}\|\mathbf{d} - \mathbf{E}(\mathbf{a})\mathbf{f}\|^2. \quad [11]$$

With the polynomial model, the encoding equation **E(a)f** can be rewritten as a linear function of the polynomial coefficients; thus Eq. [11] becomes

$$\mathbf{a} = \min_{\mathbf{a}} \frac{1}{2}\|\mathbf{d} - \mathbf{F}\mathbf{a}\|^2, \quad [12]$$

which is a standard least-squares problem where $\mathbf{F}_{[l,m],[l,i,j]} = \sum_n \rho(x_n,y_n) x_n^i y_n^j e^{-i2\pi(k_{xm}\cdot x_n + k_{ym}\cdot y_n)}$ is given. In general, the order of the polynomial used to represent the sensitivities is relatively low, so the least-squares solution can be directly obtained by

$$\mathbf{a} = (\mathbf{F}^H\mathbf{F})^{-1}\mathbf{F}^H\mathbf{d}. \quad [13]$$

The obtained polynomial coefficients are then plugged back into Eq. [6] to refine the polynomial functions of sensitivities.

MATERIALS AND METHODS

The proposed method was implemented in Matlab (MathWorks, Natick, MA, USA). To test its performance, in vivo data from a healthy volunteer were acquired on a 3T Excite MR system (GE Healthcare Technologies, Waukesha, WI, USA) using an eight-channel head coil (MRI Devices, Waukesha, WI, USA) and a 3D spoiled gradient-echo (SPGR) pulse sequence (TE = 2.38 ms, TR = 7.32 ms, flip angle = 12°, FOV = 18.7 cm × 18.7 cm, matrix = 200 × 200, slice thickness = 1.2 mm). Informed consent was obtained from the volunteer in accordance with the institutional review board policy.

The data set was acquired in full, and some phase encodings were then manually removed to simulate the VD acquisition in pMRI. The full data were combined to obtain the SoS reconstruction, which serves as a gold standard for comparison. The reduced VD data with different nominal reduction factors excluding the ACS data (R_{nom}) and different numbers of ACS lines were used to reconstruct the desired image using the proposed JSENSE method, as well as SC GSENSE (15). For different nominal reduction factors and numbers of ACS lines, the net reduction factors (R_{net}) were calculated. In JSENSE, the order of the polynomial for coil sensitivities was chosen to be $N = 17$. In SC GSENSE, the coil sensitivities were carefully estimated from the central ACS lines using the method described in Ref. 8. Briefly, the ACS data were apodized using a Kaiser window with a window shape parameter of 4, followed by the sensitivity estimation formulated in Eq. [1]. The obtained sensitivity map was then smoothed by

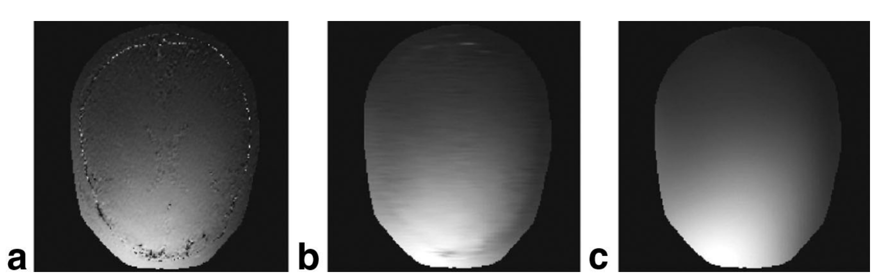

FIG. 1. Estimated sensitivity maps of the first channel based on (**a**) full-scan data, (**b**) SC with 32 ACS lines, and (**c**) JSENSE with 32 ACS lines and $R_{nom} = 4$.

Table 1
NMSEs of Sensitivity Weighted Images From Eight Channels

	Channels							
	1	2	3	4	5	6	7	8
JS (%)	5.37	5.46	4.96	4.45	4.67	4.72	4.53	4.59
SC (%)	5.99	6.01	5.48	5.02	5.05	5.17	5.06	5.11

polynomial fitting as described in Ref. 6 before it was used for GSENSE reconstruction. For comparison, the standard sensitivity map from the full-scan data was also generated using Eq. [1] followed by the same polynomial fitting procedure.

The estimated sensitivity maps, the corresponding *g*-maps, and the final reconstructions obtained by SoS, JSENSE, and GSENSE were evaluated visually in terms of image quality (e.g., noise and artifacts). With SoS as the gold standard, reconstructions were also compared quantitatively in terms of the normalized mean squared error (NMSE). The NMSE is defined as the normalized difference square between the reconstructed image ($I_{\text{estimated}}$) and the SoS as the gold standard (I_{standard}):

$$\text{NMSE} = \frac{\sum_{\vec{r}} \| I_{\text{estimated}}(\vec{r})| - |I_{\text{standard}}(\vec{r})\|^2}{\sum_{\vec{r}} |I_{\text{standard}}(\vec{r})|^2}. \qquad [14]$$

This definition is equivalent to the artifact power (AP) defined in Ref. 8. As noted in Ref. 8, a higher value of NMSE (or AP) represents reduced image quality, which suggests both increased image artifacts and noise. In addition, the sensitivity estimation errors were also calculated using Eq. [14], where we used the SoS weighted by the estimated sensitivity map for $I_{\text{estimated}}$ and the SoS weighted by the standard sensitivity map calculated from the full scan for I_{standard}. We did not subtract the estimated and standard sensitivity maps directly because the standard one is not exactly accurate due to noise amplification of division in Eq. [1], which is especially serious in the regions where the full-scan image has low intensity. Subtracting the sensitivity-weighted SoS gives more insight because the subtraction gives zero if the estimated sensitivity is accurate.

RESULTS

Figure 1a–c show the estimated sensitivity maps of the first channel based on the full scan data, the 32 ACS lines using the SC method, and the proposed JSENSE (JS) method with $R_{\text{nom}} = 4$. The sensitivity map estimated from the full scan has spatially dependent noise that is large at the skull area, where the image intensity is low. The SC method generates a map that is less noisy but has a truncation effect. The map estimated by JSENSE visually agrees with the smooth variation of the electromagnetic field with no noise or truncation effect. The qualitative

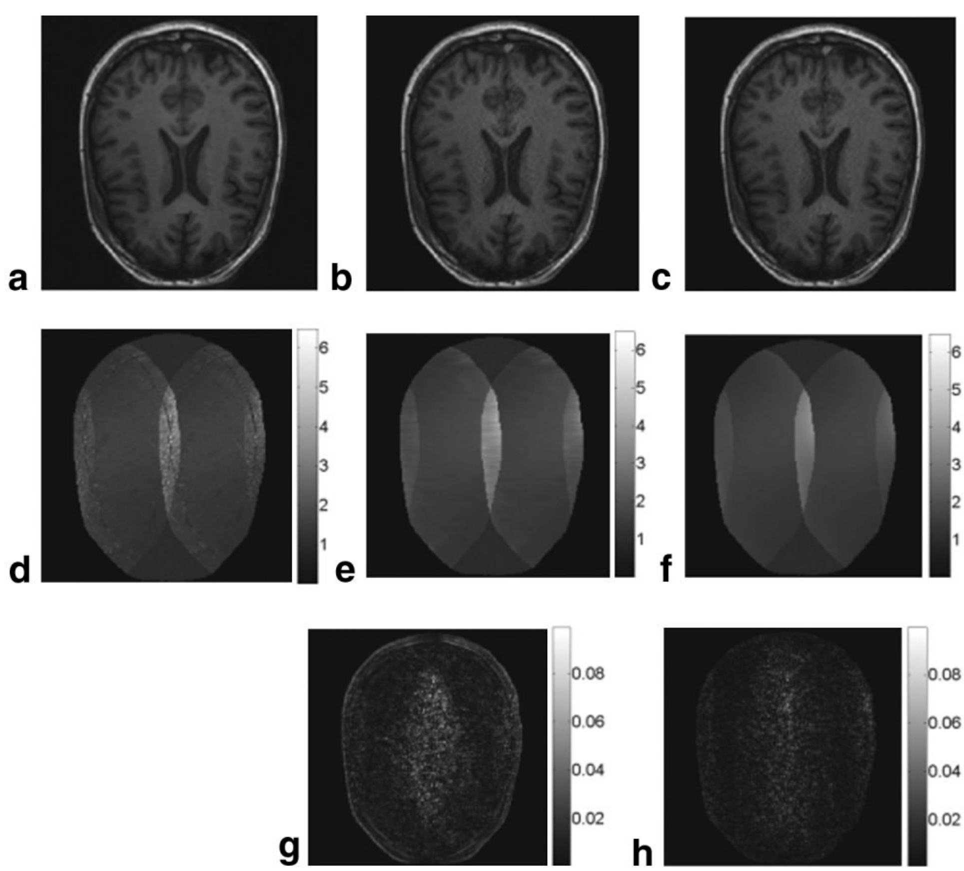

FIG. 2. The first row shows the reconstructed brain images from a set of eight-channel VD data using (**a**) SoS, (**b**) SC GSENSE, and (**c**) the proposed JSENSE. The nominal reduction factor is 3 with 32 ACS lines at the central *k*-space. Their *g*-maps are also shown on the second row corresponding to the sensitivities from (**d**) full-scan data, (**e**) SC, and (**f**) JSENSE. The difference maps between (**g**) SC GSENSE and SoS reconstructions, and (**h**) JSENSE and SoS reconstructions are shown on the third row.

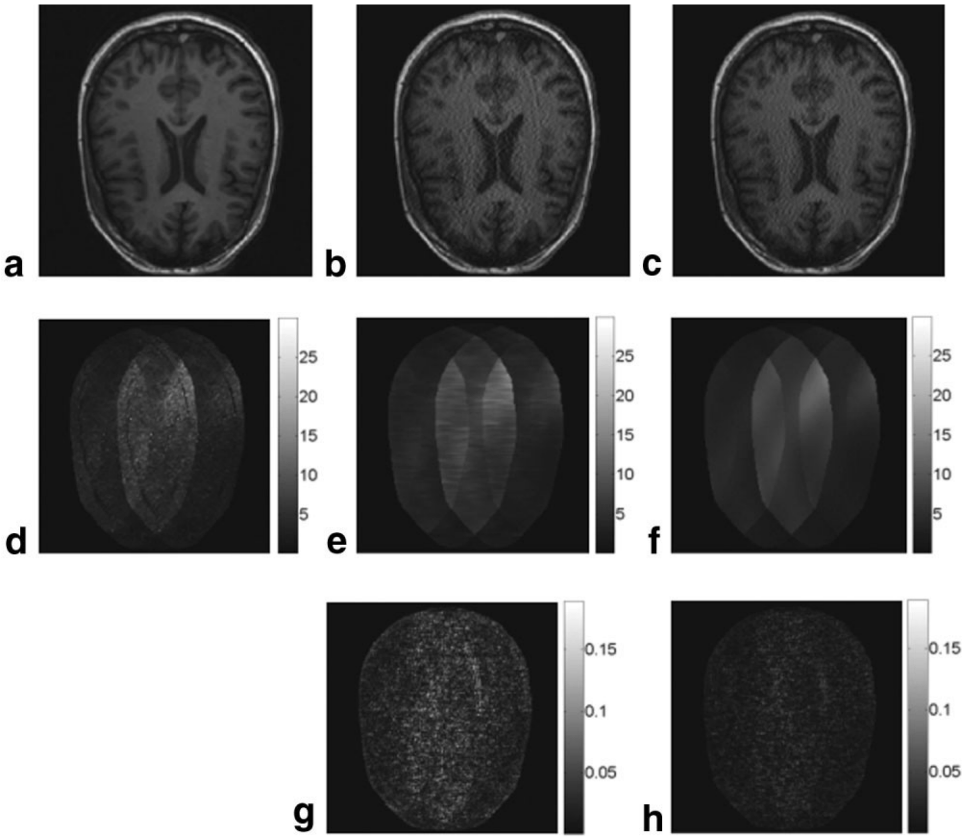

FIG. 3. The set of results with the same parameters as in Fig. 2 except that the nominal reduction factor is 5.

evaluation of these sensitivity errors for all eight channels is given in Table 1. The error for the sensitivity map from the full scan is zero, as expected, and thus is not shown. The comparison suggests that the JSENSE method improves the accuracy of the sensitivities through iterations.

Figure 2a–c show the reconstructed images using the SoS, SC GSENSE, and proposed JSENSE methods also with 32 ACS lines and $R_{nom} = 3$ ($R_{net} = 2.27$), and Fig. 2d–f show the corresponding *g*-maps. Note that the *g*-maps are shown for comparison only, and they do not reflect the actual noise enhancement in the GSENSE- and JSENSE-reconstructed images because the ACS data are used in both cases and the conjugate gradient method has an inherent regularization effect. All images are normalized and shown on the same scale. It can be seen that JSENSE is superior to SC GSENSE due to more accurate sensitivities. This can be seen more clearly in the difference image with SoS in Fig. 2g and h. The same set of comparison for 32 ACS lines and $R_{nom}= 5$ ($R_{net} = 3.05$) is given in Fig. 3, which also demonstrates the superior image quality of JSENSE.

The NMSEs (with the SoS reconstruction as the gold standard) of the SC GSENSE and JSENSE reconstructions are compared in Table 2 with columns representing the numbers of ACS lines and rows representing the nominal reduction factors. The net reduction factors are also shown in the table. For small ($R_{net} < 2.03$) or large ($R_{net} > 3.75$) net reduction factors, all methods achieve similar good or poor visual quality; thus the NMSEs in these cases may provide little insight and are not included here. The results suggest that the proposed method is preferred when a rather large data reduction is desired.

As an iterative technique, the convergence behavior of JSENSE is also studied. In Fig. 4a and b, the NMSE is plotted as a function of the number of iterations for different numbers of ACS lines and different nominal reduction factors. It shows that JSENSE converges rather quickly for all cases.

Table 2
NMSEs of Reconstructions From Brain Data

ACS	$R_{nom} = 3$			$R_{nom} = 4$			$R_{nom} = 5$			$R_{nom} = 6$		
	R_{net}	JS (%)	GS (%)	R_{net}	JS (%)	GS (%)	R_{net}	JS (%)	GS (%)	R_{net}	JS (%)	GS (%)
24	2.4	0.41	0.67	2.9	0.91	1.40	3.4	1.29	2.29	3.8	1.73	3.31
32	2.3	0.36	0.56	2.7	0.69	1.13	3.1	1.08	2.06	3.3	1.54	2.73
40	2.1	0.32	0.49	2.5	0.60	0.99	2.8	0.97	1.71	3.0	1.39	2.68
48	2.0	0.29	0.41	2.3	0.52	0.86	2.6	0.87	1.49	2.7	1.25	2.46

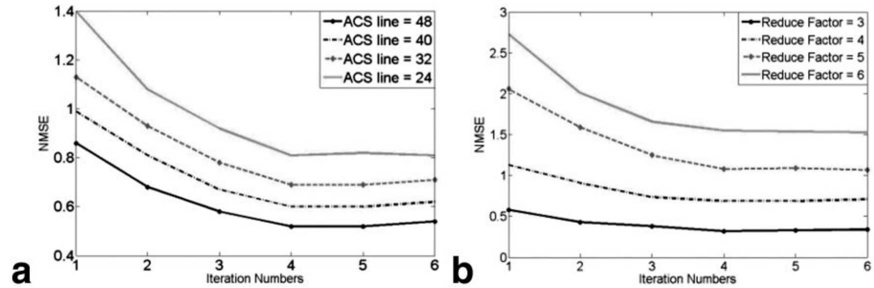

FIG. 4. NMSE vs. number of iterations in JSENSE for (**a**) different ACS lines when $R_{nom} = 4$, and (**b**) different R_{nom} with 32 ACS lines.

DISCUSSION

The proposed JSENSE method is an extension of the SC technique in the image domain (8). In particular, JSENSE is able to address two problems that arise in the existing image-domain SC technique when a large number of phase encodings are skipped for high acceleration. First, when a small number of ACS data are used for sensitivity estimation, these data are truncated from the original full data with a small truncation window, which causes the estimated sensitivities to have serious ringing at object boundaries. The erroneous sensitivities, when directly applied to a reconstruction algorithm, lead to aliasing artifacts in the final reconstruction. In JSENSE, the iterative update of the coil sensitivities implicitly takes advantage of the subsampled data from outer *k*-space in addition to the ACS data so that the truncation error in sensitivity is reduced. Second, when a large reduction factor is used, the *g*-factor is deteriorated by the inaccurate sensitivities, which leads to poor SNR in the reconstruction. The problem is alleviated by JSENSE because the iterative cross-validation regularizes the sensitivity functions such that the *g*-factor is improved.

A major limitation of JSENSE is that it exhibits a large computational complexity. Each iteration of JSENSE requires a complete GSENSE reconstruction and sensitivity estimation. The GSENSE reconstruction can be replaced by any other methods applicable to VD acquisition, and because of the separability of VD data, it can be decomposed to several 1D reconstructions. In contrast, sensitivity estimation has to be carried out in two dimensions because of the 2D parametric model, and thus dominates the computational complexity of the JSENSE method. Its computation increases with the order of the polynomial model. For an order-N polynomial, the number of unknown coefficients to be solved is $L(N + 1)^2$ (where L is the number of coils), and therefore it requires $O(L^3N^6$ computations to solve the linear equation for the coefficients. For the brain data, the running time of JSENSE is 510 s per iteration, in contrast to 36 s for GSENSE on an Intel Pentium IV 1.3 GHz desktop. Although the computational burden may present a difficulty in practice (especially in 3D imaging, due to the increased number of coefficients for a 3D polynomial), the burden may be alleviated by optimizing the code implementation of JSENSE. In addition, as computers become faster, the computational speed may be of less concern than the data acquisition speed.

Reformulation of the image reconstruction problem in the context of joint estimation presents appealing possibilities for future research. For example, models other than the polynomial one may be investigated to accurately represent the spatial variation of coil sensitivities with fewer model coefficients to be solved. Other optimization algorithms, such as variable projection, may be applied to improve computational efficiency. The use of a VD acquisition pattern other than the one used in this paper may also improve the quality of JSENSE reconstruction under a given net acceleration factor (20). In addition, it would also be of great interest to generalize JSENSE to non-Cartesian trajectories, such as spiral and radial trajectories. These trajectories automatically sample the center of *k*-space densely such that central *k*-space automatically satisfies the Nyquist sampling rate even with reduced encoding.

CONCLUSIONS

We have demonstrated a novel pMRI-reconstruction method with improved self calibration of coil sensitivities. The method iteratively refines the sensitivities so that the SNR of reconstruction is improved and the image artifact is reduced. The proposed JSENSE method is expected to improve the image reconstruction quality in dynamic parallel imaging applications because of its ability to accurately update the continuously changing sensitivities, as well as its superior reconstruction quality when a large net acceleration factor is used to reduce motion artifacts due to long acquisition times.

ACKNOWLEDGMENT

The authors thank Dr. Z-P Liang for valuable discussions nd Dr. Y. Xu for help with data.

REFERENCES

1. Griswold MA, Jakob PM, Nittka M, Goldfarb JW, Haase A. Partially parallel imaging with localized sensitivities (PILS). Magn Reson Med 2000;44:602–609.
2. Jakob PM, Griswold MA, Edelman RR, Sodickson DK. AUTO-SMASH: a self-calibrating technique for SMASH imaging. MAGMA 1998;7:4254.
3. Heidemann RM, Griswold MA, Haase A, Jakob PM. VD-AUTO-SMASH imaging. Magn Reson Med 2001;45:1066–1074.
4. Griswold MA, Jakob PM, Heidemann RM, Mathias Nittka, Jellus V, Wang J, Kiefer B, Haase A. Generalized autocalibrating partially parallel acquisitions (GRAPPA). Magn Reson Med 2002;47:1202-1210.
5. Sodickson DK, Manning WJ. Simultaneous acquisition of spatial harmonics (SMASH): fast imaging with radiofrequency coil arrays. Magn Reson Med 1997;38:591–603.
6. Pruessmann KP, Weiger M, Scheidegger MB, Boesiger P. SENSE: sensitivity encoding for fast MRI. Magn Reson Med 1999;42:952–962.

7. Kyriakos WE, Panych LP, Kacher DF, Westin C-F, Bao SM, Mulkern RV, Jolesz FA. Sensitivity profiles from an array of coils for encoding and reconstruction in parallel (SPACE RIP). Magn Reson Med 2000;44:301–308.
8. McKenzie CA, Yeh EN, Ohliger MA, Price MD, Sodickson DK. Self-calibrating parallel imaging with automatic coil sensitivity extraction. Magn Reson Med 2002;47:529-538.
9. Kellman P, Epstein FH, McVeigh ER. Adaptive sensitivity encoding incorporating temporal filtering (TSENSE). Magn Reson Med 2001;45: 846-852.
10. Madore B. UNFOLD-SENSE: a parallel MRI method with self-calibration and artifact suppression. Magn Reson Med 2004;52:310-320.
11. Madore B, Glover GH, Pelc NJ. Unaliasing by Fourier-encoding the overlaps using the temporal dimension (UNFOLD) applied to cardiac imaging and fMRI. Magn Reson Med 1999;42:813–828.
12. Lin F-H, Kwong KK, Belliveau JW, Wald LL. Parallel imaging reconstruction using automatic regularization. Magn Reson Med 2004;51: 559–567.
13. Yuan L, Ying L, Xu D, Liang Z-P. Truncation effects in SENSE reconstruction. Magn Reson Imaging 2006;24:1311–1318.
14. Lin F-H, Chen Y-J, Belliveau JW, Wald LL. A wavelet-based approximation of surface coil sensitivity profiles for correction of image intensity inhomogeneity and parallel imaging reconstruction. Hum Brain Mapp 2003;19:96–111.
15. Pruessmann KP, Weiger M, Böernert P. Advances in sensitivity encoding with arbitrary k-space trajectories. Magn Reson Med 2001;46:638–651.
16. Sutton BP, Noll DC, Fessler JA. Dynamic field map estimation using a spiral-in/spiral-out acquisition. Magn Reson Imaging 2004;51:1194–1204.
17. Samsonov AA, Kholmovski EG, Parker DL, Johnson CR. POCSENSE: POCS-based reconstruction method for sensitivity encoded magnetic resonance imaging. Magn Reson Med 2004;52:1397–1406.
18. Ying L, Xu D, Liang Z-P. On Tikhonov regularization for image reconstruction in parallel MRI. In: Proceedings of the 26th Annual International Conference of IEEE EMBS, San Francisco, CA, USA, 2004. p 1056–1059.
19. King KF. Efficient variable density SENSE reconstruction. In: Proceedings of the 13th Annual Meeting of ISMRM, Miami Beach, FL, USA, 2005 (Abstract 2418).
20. Xu D, Ying L, Jacob M, Liang Z-P. Optimizing SENSE for dynamic imaging. In: Proceedings of the 13th Annual Meeting of ISMRM, Miami Beach, FL, USA, 2005 (Abstract 2419).